Adhesion Energy of Receptor-Mediated Interaction Measured by Elastic Deformation

Vincent T. Moy,* Yuekan Jiao,* Thomas Hillmann,* Horst Lehmann,# and Takeshi Sano§

*Department of Physiology and Biophysics, University of Miami School of Medicine, Miami, Florida 33136 USA; #Physik Department, Biophysics Group, Technische Universität München, 8046 Garching, Germany; and §Center for Molecular Imaging, Diagnosis and Therapy, Department of Radiology, Beth Israel Deaconess Medical Center, Harvard Medical School, Boston, Massachusetts 02215 USA

ABSTRACT We investigated the role of receptor binding affinity in surface adhesion. A sensitive technique was developed to measure the surface energy of receptor-mediated adhesion. The experimental system involved a functionalized elastic agarose bead resting on a functionalized glass coverslip. Attractive intersurface forces pulled the two surfaces together, deforming the bead to produce an enlarged contact area. The Johnson-Kendall-Roberts (JKR) model was used to relate the surface energy of the interaction to the elasticity of the bead and the area of contact. The surface energies for different combinations of modified surfaces in solution were obtained from reflection interference contrast microscopy (RICM) measurements of the contact area formed by the bead and the coverslip. Studies with surfaces functionalized with ligand-receptor pairs showed that the relationship between surface energy and the association constant of the ligand binding has two regimes. At low binding affinity, surface energy increased linearly with the association constant, while surface energy increased logarithmically with the association constant in the high affinity regime.

INTRODUCTION

Cell-cell and cell-substrate interactions play a crucial role in regulation and development of the immune system (Springer, 1990, 1994). Cell adhesion appears to be a dynamic process (Diamond and Springer, 1994), mediated by the specific interactions of adhesion molecules on apposing cell membranes. Among their diverse functions, adhesion molecules direct the homing of lymphocytes to targeted tissues and mediate the transient interactions of antigen-infected cells and T lymphocytes. Apparently, the shear force exerted by the bloodstream is sufficient to rupture the bonds formed at the rear of the cells to drive the lymphocytes to roll downstream, but insufficient to dislodge the cells (Lawrence and Springer, 1991; Lauffenburger and Howitz, 1996). The dynamic properties of the adhesion molecules also play an important role in stabilizing the interaction between T cells and antigen presenting cells (APC). Here, cell adhesion is regulated by the transient interaction between lymphocyte function-associated antigen-1 (LFA-1), an integrin expressed on the T cell surface, and intercellular adhesion molecule 1 (ICAM-1) on the APC (Dustin and Springer, 1989).

Several factors contribute to the strength of cell adhesion including binding affinity of the adhesion molecules, receptor density, receptor-cytoskeleton interaction, cytoskeletal reorganization, and lateral mobility of membrane receptors. In this report we will focus on the relationship between binding affinity of ligand-receptor interaction and mechanical strength of cell adhesion. Recent studies carried out in a cell-free model system have shown that adhesion strength is a linear function of the free energy of receptor binding, i.e., the logarithm of the affinity constant (Kuo and Lauffenburger, 1993). Although these measurements are consistent with theoretical models (Dembo et al., 1988; Evans, 1985), they failed to explain some experimental observations. In particular, the adhesion of T cells to an ICAM-1-coated substrate increased by 100-fold upon activation of the T cell, even though only a small fraction of LFA-1 was converted to a higher affinity state (Lollo et al., 1993).

The ability to directly measure the strength of weakly adherent surfaces is necessary for determining the biophysical mechanisms of cell adhesion. Direct force measurements of biomolecular adhesion have been obtained by using a number of different techniques. The biotin-avidin interaction has been studied in detail by atomic force microscopy (AFM) and the surface force apparatus (Florin et al., 1994; Leckband et al., 1994; Moy et al., 1994; Lee et al., 1994; Chilkoti et al., 1995a). Adhesion between individual cells was measured using a micropipette technique (Tözeren et al., 1992; Evans et al., 1991; Sung et al., 1992). Another commonly used technique measures the critical shear stress for the detachment of bound cells or functionalized beads from a chemically defined substrate (Kuo and Lauffenburger, 1993; Lawrence and Springer, 1991). All of these approaches measure adhesion in terms of the mechanical force needed to induce surface separation and, hence, depend on the detachment mechanism.

Here we report on the development and application of a novel thermodynamic approach for measuring adhesion based on the free energy change associated with separation of two solid surfaces in contact. A glass slide and an elastic agarose bead provided the two functionalized surfaces to be

Received for publication 17 August 1998 and in final form 8 December 1998.

Address reprint requests to Dr. Vincent T. Moy, Department of Physiology and Biophysics, University of Miami School of Medicine, 1600 N.W. 10th Avenue, Miami, FL 33136. Tel.: 305-243-3201; Fax: 305-243-5931; E-mail: vmoy@newssun.med.miami.edu.

0006-3495/99/03/1632/07 $2.00

tested. The technique is based on the JKR model, which relates the surface energy to the induced deformation of the elastic sphere (Johnson et al., 1971). In the initial application of the technique, we examined the interactions between two oppositely charged surfaces in solution. Next, the avidin-biotin pair was used as a model system for specific molecular adhesion (Green, 1975). Several attributes made the biotin-avidin system ideal for this research. The avidin-biotin complex has been well-characterized by multiple biochemical and physical methods (Weber et al., 1989; Livnah et al., 1993; Chilkoti and Stayton, 1995), and thus facilitates the interpretation of the surface energy measurements. Avidin binds to biotin with high affinity and specificity. In addition to its naturally occurring homolog, streptavidin, there exist streptavidin mutants that bind to biotin analogs over a range of affinity constants (Green, 1966, 1990; Sano and Cantor, 1995; Chilkoti et al., 1995b).

MATERIALS AND METHODS

Measurements of contact surfaces

RICM was used to measure the contact radius formed by the agarose bead resting on the glass coverslip (Gingell and Todd, 1979). Fig. 1 *A* illustrates the principle of RICM. A Zeiss Axiovert 135 microscope equipped with a Neofluar 63/1.25 Antiflex objective (Zeiss, Jena, Germany) was modified for the RICM measurements. Polarized light waves reflected from the upper glass surface (I_1) and the surface of the bead (I_2) interact to create an interference image. The intensity at a given position in the image depends on the separation $h(x)$ between the two surfaces:

$$I(x) = I_1 + I_2 + 2\sqrt{I_1 I_2}\cos[2kh(x) + \delta], \qquad (1)$$

where $k = 2\pi n/\lambda$, and n and λ are the index of refraction of the buffer and the wavelength of the monochromatic light, respectively (Rädler and Sackmann, 1992). Since the refraction index of the bead is higher than that of the buffer, the phase shift δ is π. In order to detect the interference pattern, stray light was reduced by an antiflex technique. This is accomplished with a $\lambda/4$-plate placed between the sample and the objective lens, and crossed polarizers in the illumination and observation paths of light. In the region of contact, corresponding to $h(x) = 0$ and $I(x) = I_1 + I_2 - 2\sqrt{I_1 I_2}$, the intensity of the image is at its minimum (see Fig. 1 *B*). The RICM image was captured with a CCD camera (Hamamatsu C5985), digitized by an Apple PowerMac 8500 computer, and analyzed with NIH Image 1.60 and Igor Pro software (WaveMetrics, Inc., Lake Oswego, OR) to obtain the area of the contact region, a.

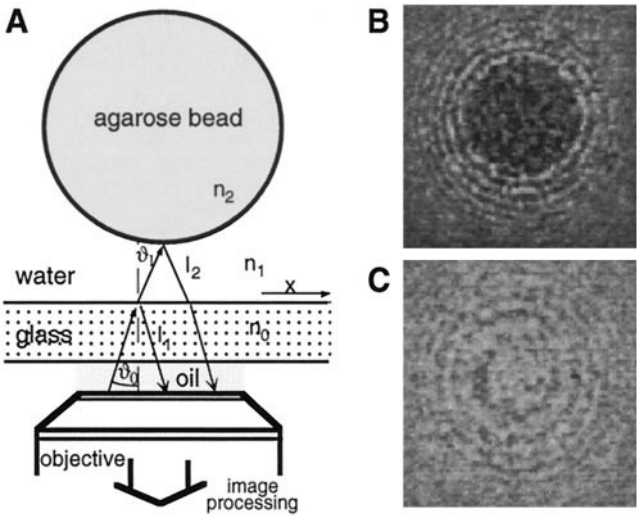

FIGURE 1 (*A*) Schematics of reflection interference contrast microscopy. RICM images of iminobiotin derivatized 4% agarose beads on (*B*) glass and (*C*) a MgF_2 modified glass coverslip.

Elasticity measurements of agarose beads

Young's modulus of the agarose beads was determined by AFM (Binnig et al., 1986). A tipless cantilever (Digital Instrument, Santa Barbara, CA) was used in the force scan measurements over the center of the agarose beads. The force-indentation curve of elastic beads was obtained from the AFM measurement using the glass substrate to calibrate the deflection of the cantilever (Radmacher et al., 1996). The relation between force F and indentation δ is given in the Hertz model as:

$$F = \frac{4E\sqrt{R}}{3(1 - \nu^2)}\,\delta^{3/2}, \qquad (2)$$

where E, ν, and R are Young's modulus, the Poisson ratio, and the radius of the bead, respectively. Young's modulus of the biotin and iminobiotin beads, as determined by nonlinear regression analysis (Igor Pro) of >10 force-indentation curves, were 7.6×10^4 N/m^2 and 9.3×10^4 N/m^2, respectively. For a given type of bead, Young's modulus of individual beads for all bead sizes did not vary by >5%. The Poisson ratio was taken to be 0.5. The radius of the beads was measured by light microscopy. The spring constant of the tipless cantilevers used in the force scan measurements was obtained from thermal fluctuation analysis of the cantilever (Hutter and Bechhoefer, 1994; Florin et al., 1995).

Sample preparation

Biotin-linked and iminobiotin-linked agarose beads (4% agarose, non-cross-linked) were purchased from Sigma (St. Louis, MO). The beads were washed four times with water or buffer. All solutions were prepared with water purified by the Nanopure UV filtration system (Barstead, Dubuque, IA). Buffers were prepared from the purest grade reagents available. A deglycosylated form of avidin (NeutrAvidin) was used in the experiments. Both streptavidin and NeutrAvidin were purchased from Pierce (Rockford, IL) and used without further purification. Stv38 is a truncated form of streptavidin (aa. 16–133) with a substitution at residue 120 (Trp to Phe). Expression and purification of stv38 were described elsewhere (Sano and Cantor, 1995).

Coverslips were functionalized with avidin as follows: optical round flat glass coverslips (VWR Micro Cover Glasses, 25 mm diameter, 0.13–0.17 mm thick) were cleaned in boiling 2% RBS-35 detergent (Pierce) solution for 15 min, sonicated for 30 min, rinsed vigorously with deionized water, and dried at 40°C. The cleaned coverslips were silanized with 2% v/v 3-aminopropyltriethoxysilane (Sigma Chemical) in acetone under constant agitation for 10 min. The silanized coverslips were rinsed with deionized water and subsequently immersed in 0.1% glutaraldehyde (Sigma) for 30 min at room temperature. The coverslips were removed from the glutaraldehyde solution, rinsed with deionized water, and incubated in 2 ml avidin solution (50 μg/ml) for 2 h at room temperature to generate the avidin functionalized surface. To block remaining aldehyde groups on the glass surface, the coverslips were treated with 0.2 M glycine and rinsed with phosphate buffered saline (PBS, 10 mM PO_4^{-3}, 150 NaCl, pH 7.3). The coverslips were stored up to 3 days in PBS containing 0.1% azide and 0.5% BSA at 4°C. The same procedure was used to functionalize coverslips with the avidin homologs.

RESULTS

The interaction of two elastic spheres is given in the JRK model (Israelachvili, 1992; Johnson et al., 1971). In the

special case of an elastic sphere pressed against a hard flat surface with a force F (see Fig. 2), the radius a of the contact area is given by

$$a^3 = \frac{R}{K}(F + 3\pi RW + \sqrt{6\pi RWF + (3\pi RW)^2}), \quad (3)$$

where R is the radius of the sphere, $K = [4E/3(1 - \nu^2)]$ is the effective elastic modulus of the sphere, and W is the surface energy. If the external force acting on the sphere is negligible, the surface energy and contact radius are related by

$$a^3 = 6\pi \frac{W}{K} R^2 \quad (4)$$

Hence, the surface energy of adhesion can be derived from measurements of the contact radius, provided that Young's modulus of the sphere is known.

Surface energy of charged surfaces in solution

To test the applicability of the JKR model in our experimental system, we investigated the interaction of iminobiotin-functionalized agarose beads resting on the surface of a glass coverslip in water. The contact radius formed by the iminobiotin bead and the glass substrate was measured by RICM. Fig. 1 illustrates the principle of RICM and shows RICM images of an iminobiotin bead on glass (*B*) and on a glass surface modified by MgF_2 via vapor deposition (*C*). The contact between the iminobiotin bead and the glass substrate was detected as a dark disk surrounded by a series of concentric rings (Fig. 1 *B*). The center disk corresponds to the area of contact and the rings are the interference pattern formed by polarized light reflected from the upper surface of the coverslip and the surface of the bead. The contact radii formed by beads of different sizes were measured and plotted against the bead radius in Fig. 3. We fitted the data with a power function $R = C_1 a^{C_2}$, and the value of C_2, as determined by nonlinear regression using GraphPad Prism (San Diego, CA), was 1.5 ± 0.1. This result demonstrates that the JKR model is applicable to the experimental system and that the contribution from external forces (i.e., gravity) is negligible; otherwise C_2 would have deviated from 1.5 predicted by the model. The surface energy obtained by fitting the data (Fig. 3) to Eq. 4 with E = 93,000 N/m^2 was 1.0 ± 0.03 mJ/m^2.

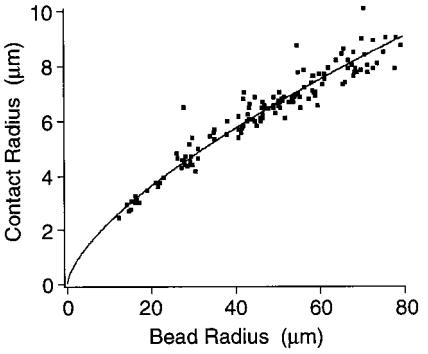

FIGURE 3 Contact radius versus bead radius of iminobiotin functionalized 4% agarose beads on a glass coverslip in water.

Adhesion of the iminobiotin beads to the coverslip can be attributed to electrostatic interactions between the positively charged guanidino group of iminobiotin and the negatively charged oxide groups of the glass surface. To test this assertion, we carried out measurements over a range of electrolyte concentrations (see Fig. 4 *A*). The rapid decay in surface energy with increasing NaCl concentration is consistent with the shielding of surface charges as described in

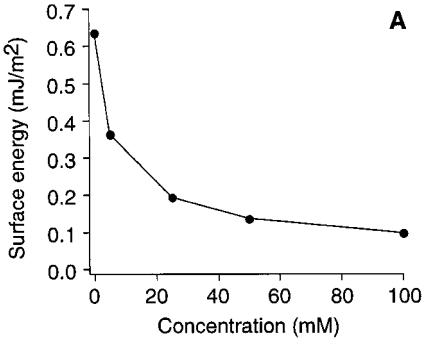

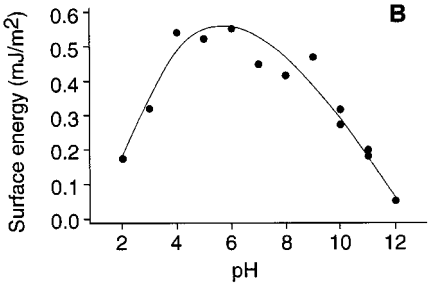

FIGURE 4 (*A*) Ionic strength-dependence of surface energy of iminobiotin beads on glass. Measurements were made at different NaCl concentrations in 1 mM Tris, pH 8. (*B*) pH dependence of surface energy of iminobiotin beads on glass in 2 mM sodium phosphate. Each data point was derived from nonlinear regression analysis of >50 measurements.

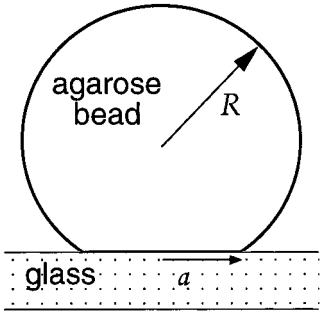

FIGURE 2 Schematic of the JKR model for interaction between an elastic agarose bead of radius R and a rigid flat substrate. The contact radius a is a function of the bead radius, surface energy W, and elastic modulus of the bead K.

the DLVO theory. The interaction between the iminobiotin beads and the glass substrate also exhibited pH dependence (Fig. 4 *B*). The adhesion detected within the pH range of 5 to 12 can be attributed to the ionization of the surfaces. At pH above the pK of the guanidino group (11.95) adhesion energy decreased due to the neutralization of surface charges on the bead (Green, 1966), while in the pH range below 5, the silanol groups on the glass surface are neutralized and hence the adhesion energy decreased. There remained some adhesion even at the extremes of pH and electrolyte concentrations that can be attributed to van der Waals forces.

Surface energy of specific interaction

The surface energy of the specific interaction between avidin and biotin functionalized surfaces in PBS was obtained from the elastic deformation measurements. In these measurements, avidin was immobilized on glass coverslips while biotin was covalently attached to agarose beads. The total surface energy includes both the specific interaction of the avidin-biotin complex and nonspecific interaction between the substrates. To obtain the fraction of the surface energy attributable to the specific binding of avidin to biotin, the nonspecific contribution was determined after introducing 1 μM of free *d*-biotin into the solution. The total surface energy, obtained from the analysis of >50 measurements, was 200 $\pm$ 9 μJ/m^2. The specific surface energy of a biotin bead interacting with the avidin-coated coverslip was 162 $\pm$ 9 μJ/m^2. The surface energies of other ligand-receptor systems are listed in Table 1. The streptavidin-biotin pair exhibited surface energy similar to the biotin-avidin pair. The biotin-stv38 and iminobiotin-avidin interactions both had lower surface energy, following the pattern of binding affinity.

To study the relationship between surface energy and binding affinity further, we measured the surface energy mediated by the interaction between iminobiotin and avidin. Iminobiotin contains an ionizable guanidino group and thus can exist in a neutral or protonated form. Avidin binds strictly to the neutral form of iminobiotin. Hence, the binding affinity of the avidin-iminobiotin complex is pH-dependent (Green, 1966). The association constant of the iminobiotin-avidin pair increases monotonically with pH of the buffer. We used this pH dependence to study the relationship between the surface energy of the ligand-receptor interaction and binding affinity. Surface energy measurements of the iminobiotin-avidin interface were carried out from pH 5 to 12 (Fig. 5 *A*). The surface energy measurements were complicated by a nonspecific contribution that presumably stemmed from the positively charged iminobiotin bead and residual negative charges on the glass. At pH <5, the nonspecific surface energy is >30 μJ/m^2 and sta-

TABLE 1 Surface energy of ligand-receptor interactions

Ligand-receptor	W_{tot} (μJ/m^2)	$W_{non\text{-}sp}$ (μJ/m^2)	W_{sp} (μJ/m^2)	K_d (M)
Biotin-avidin	200 $\pm$ 9	38 $\pm$ 2	162 $\pm$ 9	10^{-15}
Biotin-streptavidin	168 $\pm$ 3	negligible	168 $\pm$ 3	10^{-15}
Biotin-stv38	85 $\pm$ 1.4	52 $\pm$ 1.6	33 $\pm$ 1.6	10^{-8}
Iminobiotin-avidin	48 $\pm$ 1.2	19 $\pm$ 0.8	29 $\pm$ 1.2	4.4 $\times 10^{-7}$

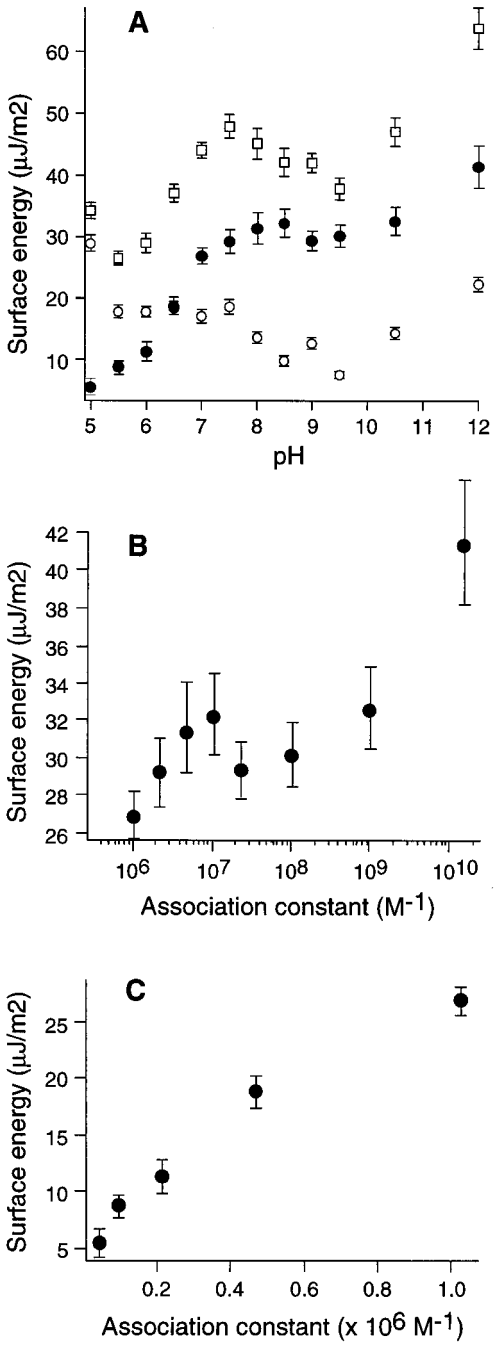

FIGURE 5 (*A*) pH dependence of surface energy. Surface energy measurements were carried out with iminobiotin-functionalized beads on an avidin-coated substrate over the pH range of 5 to 12. The specific surface energy (●) was derived from difference of the total surface (■) and nonspecific surface energy (○). Specific surface energy versus equilibrium binding affinity plots in (*B*) high affinity regime and (*C*) low affinity regime. Each data point was derived from nonlinear regression analysis of >50 measurements.

tistically indistinguishable from the total surface energy (data not shown). To obtain the specific surface energy, the nonspecific surface energy was determined by blocking the avidin molecules on the glass surface with excess free *d*-biotin. Fig. 5, *B* and *C* show the correlation between specific surface energy and equilibrium association constant K_a of the iminobiotin-avidin interaction. The pH dependence of the affinity was previously measured by Green (1990). In the high affinity regime ($K_a > 10^6\ M^{-1}$; pH >7), surface energy increased linearly with the logarithm of K_a (Fig. 5 *B*). In the low affinity regime at pH <7, surface energy increased linearly with K_a (Fig. 5 *C*).

DISCUSSION AND CONCLUSIONS

A theoretical upper limit on the surface energy of the biotin-avidin interaction can be obtained on the assumption that every avidin binds to a biotin and contributes 35 kT to the surface energy (Green, 1990). If the glass surface is densely packed with a receptor density of 2×10^{16} avidin/m^2, the estimated surface energy is 2.8 mJ/m^2, which is an order of magnitude larger than our measured value. This discrepancy can be attributed to an incomplete coverage of the surface with receptor, a diminished activity of bound receptor, and the surface roughness of the agarose bead which prevented complete contact of the two surfaces. The roughness of agarose bead on the micrometer scale is evident in high magnification light microscopy images of the beads and by graininess in the contact area observed in interference contrast images of the beads in contact with the substrate (Fig. 1 *B*).

While there are incompatibilities between the measured and predicted surface energy values, the elastic deformation measurements do provide an opportunity to examine the surface energy of related systems. Of particular interest in the current study is how surface energy varies with the equilibrium binding affinity. This analysis does not require knowledge of the receptor coverage of the substrates nor the fraction of the bead surface accessible to contact formation. To permit direct comparison of surface energy with changes in binding affinity, we designed an experimental system that permitted us to change binding affinity without having to change the ligand or the receptor. This can be achieved in the avidin-iminobiotin system, which exhibits a 6-order-of-magnitude increase in affinity between pH 5 and 12 (Green, 1966). Above pH 7, the surface energy of the system increased linearly with the logarithm of the association constant (Fig. 5 *A*) as reported in similar studies (Kuo and Lauffenburger, 1993). However, the surface energy increases linearly with the association constant in the low binding affinity regime (Fig. 5 *B*) as predicted by Dembo et al. (1988).

Our measurements have revealed a direct correlation between the adhesion energy and the equilibrium dissociation of the ligand-receptor complex that is consistent with the Dembo model. According to the model, the surface energy of the interaction is given by $W = k_B T N_R \ln\{1 + (N_L/K_D)\}$, where N_R and N_L are the receptor density and ligand density, respectively, and K_D is the surface dissociation constant of the complex (Dembo et al., 1988). We will assume that the surface dissociation constant is proportional to the solution dissociation constant (i.e., $K_D = \eta K_d$). The dependence of W on K_d falls into one of two regimes. If $N_L/\eta K_d \gg 1$, then $W = k_B T N_R \ln\{N_L/\eta K_d\}$ and W scales with the logarithm of K_d and linearly with the free energy (ΔG) of the complex formation. If $(N_L/\eta K_d) \ll 1$, then $W = k_B T (N_R N_L/\eta K_d)$ and W is proportional to the binding affinity constant, K_d.

The surface energy measurements of the iminobiotin-avidin interaction reveal that the transition from a linear to a logarithmic dependence on binding affinity occurs at the K_a of $10^6\ M^{-1}$ (corresponding to pH 7). The position of the transition [i.e., $(N_L/\eta K_d) \approx 1$] provides an estimate for the proportionality constant η, which is related to the gap between the two surfaces. The surface density of iminobiotin on the agarose beads based on manufacturer information is 8×10^{18} iminobiotin/m^2, which estimates η at 8×10^{24} #-liter/m^2mol. This value is larger than a previously determined value ($\sim 10^{22}$ #-liter/m^2-mol) for an experimental system that involved 10 μm polystyrene beads in contact with a glass substrate (Kuo and Lauffenburger, 1993). This difference reflected the accessibility for receptor binding. Evidently, the smaller latex beads were able to form better contact with the glass substrate than did the agarose beads due to the surface roughness of the agarose beads.

An important application of the surface energy measurement is the analysis of cell adhesion dynamics. A survey of ligand-receptor complexes predicted to mediate cell adhesion revealed that their binding affinities are usually lower than $10^7\ M^{-1}$ (Schneck et al., 1989; Lollo et al., 1993; Nicholson et al., 1998), which is relatively low when compared to the affinity constants of antibodies for their antigens, which routinely exceed $10^8\ M^{-1}$. High binding affinities in adhesion complexes are generally thought of as unnecessary since strong adhesion can be achieved through multiple interactions. Our analysis suggests that the relative low binding affinity of adhesion complexes might actually be crucial for the regulation of cell adhesion. To support this assertion, we examined the dynamics of the LFA-1/ICAM-1 interaction in mediating cell adhesion. T cells activated by phorbol ester adhered to the ICAM-1 coated substrate via LFA-1 significantly tighter than resting T cells (Dustin and Springer, 1989). Resting T cells were dislodged with a centrifugal force of 100 pN, while activated cells were able to withstand forces of up to 10 nN (Moy, unpublished results). The enhanced adhesion was shown to be associated with a change in the affinity of LFA-1 for ICAM-1 (Lollo et al., 1993). LFA-1 on resting T cells binds to ICAM-1 with low affinity ($K_d = 6.7 \times 10^{-5}$ M). Upon activation, the T cells expressed two forms of LFA-1 with different affinities for ICAM-1. Approximately 80% of the LFA-1 remains unchanged and only 20% of the molecule showed a higher affinity for ICAM-1 ($K_d = 3.6 \times 10^{-7}$ M). Since upregu-

lation of LFA-1 and redistribution of LFA-1 to the site of contact were ruled out by fluorescence studies and lateral diffusion measurements, the enhanced adhesion upon activation is generally attributed to a change in the affinity state of LFA-1. A question that remains is whether this conclusion is consistent with theory. A 200-fold increase in the affinity constant in 20% of LFA-1 may lead to a 100-fold increase in the adhesion strength provided that binding affinity and receptor density satisfied conditions set in the Dembo model. There were ~300,000 LFA-1 expressed on the surface of the hybridoma cell line (3DO-54.8) used in the studies (Lollo et al., 1993). The diameter of the cell was ~20 μm. Assuming uniform distribution, the density of LFA-1 molecules on the cell surface was 2.4×10^{14} #/m^2. In addition to the receptor density, the relationship between surface energy and binding affinity also depends on the proportionality constant η. A theoretically calculated value of η based on an intersurface gap of 200 Å is 1.2×10^{19} #-liter/m^2-mol, which is 10^6 times smaller than the value obtained in our measurements. However, it is unlikely that our value is appropriate for the analysis of cell-cell interaction since deformability of the cell membrane permits greater access to receptor binding. We will use an intermediate value obtained by Kuo and Lauffenburger in our analysis (Kuo and Lauffenburger, 1993). For $\eta = 10^{22}$ #-liter/m^2-mol, the transition between linear and logarithmic dependence of surface energy on binding constant occurs at a K_d of 2.4×10^{-8} M, which is less than the dissociation constants of the LFA-1/ICAM-1 complex. Thus, an increase in affinity from 6.7×10^{-5} M to 3.6×10^{-7} M is expected to result in a 200-fold increase in surface energy, consistent with the 100-fold increase in adhesive strength observed experimentally. If the increase in binding affinity of ICAM-1 to LFA-1 were from 10^{-8} to 10^{-10} M instead, the predicted increase in adhesion would only be six-fold.

In this report we introduced a relatively simple approach toward obtaining the adhesion energy of specific interactions of ligand and protein immobilized on apposing surfaces. The agarose bead is an ideal elastic substrate in these measurements due to the ease in protein derivatization and the low nonspecific activity of the agarose matrix. The sensitivity of measurements is limited by the method's inability to resolve surface contact of <1 μm radius. For a bead with a radius of 50 μm and effective elastic modulus of 1.65×10^5 N/m^2, the practical detection limit of the surface energy is ~3.5 μJ/m^2. However, the sensitivity of the technique can be improved by using a more elastic substrate. For example, red blood cells could be used in place of the agarose beads. Alternatively, it might be possible to obtain surface energy measurements using rigid beads and a thin elastic gel supported on a substrate. Gels can be fabricated to have elastic properties 100 times softer than the agarose beads. These refinements should permit us to study weaker interactions than what is currently possible.

We thank M. Schmidt, T. Kuhn, T. Feder, C. Freites, and S. Sutter for technical support and A. Chen for assistance in manuscript preparation.

This work was supported by National Institutes of Health Grant 1 R29 GM55611-01 (to V.T.M.).

REFERENCES

Binnig, G., C. F. Quate, and C. Gerber. 1986. Atomic force microscope. *Phys. Rev. Lett.* 56:930–933.

Chilkoti, A., T. Boland, B. D. Ratner, and P. S. Stayton. 1995a. The relationship between ligand-binding thermodynamics and protein-ligand interaction forces measured by atomic force microscopy. *Biophys. J.* 69:2125–2130.

Chilkoti, A., and P. S. Stayton. 1995. Molecular origins of the slow streptavidin-biotin dissociation kinetics. *J. Am. Chem. Soc.* 117: 10622–10628.

Chilkoti, A., P. H. Tan, and P. S. Stayton. 1995b. Site-directed mutagenesis studies of the high-affinity streptavidin-biotin complex: contributions of tryptophan residues 79, 108, and 120. *Proc. Natl. Acad. Sci. USA.* 92:17544–11758.

Dembo, M., D. C. Torney, K. Saxman, and D. Hammer. 1988. The reaction-limited kinetics of membrane-to-surface adhesion and detachment. *Proc. R. Soc. Lond. Ser. B.* 234:55–83.

Diamond, M. S., and T. A. Springer. 1994. The dynamic regulation of integrin adhesiveness. *Curr. Biol.* 4:506–517.

Dustin, M. L., and T. A. Springer. 1989. T-cell receptor cross-linking transiently stimulates adhesiveness through LFA-1. *Nature.* 341: 619–624.

Evans, E. A. 1985. Detailed mechanics of membrane-membrane adhesion and separation. I. Continuum of molecular cross-bridges. *Biophys. J.* 48:175–183.

Evans, E., D. Berk, and A. Leung. 1991. Detachment of agglutinin bonded red blood cells. I. Forces to rupture molecular point attachments. *Biophys. J.* 59:838–848.

Florin, E.-L., V. T. Moy, and H. E. Gaub. 1994. Adhesive forces between individual ligand-receptor pairs. *Science.* 264:415–417.

Florin, E.-L., M. Rief, H. Lehmann, M. Ludwig, C. Dornmair, V. T. Moy, and H. E. Gaub. 1995. Sensing specific molecular interactions with the atomic force microscope. *Biosensor Bioelectron.* 10:895–901.

Gingell, D., and I. Todd. 1979. Interference reflection microscopy: a quantitative theory for image interpretation and its application to cell-substratum separation measurements. *Biophys. J.* 26:507–526.

Green, N. M. 1966. Thermodynamics of the binding of biotin and some analogues by avidin. *Biochem. J.* 101:774–780.

Green, N. M. 1975. Avidin. *Adv. Protein Chem.* 29:85–133.

Green, N. M. 1990. Avidin and streptavidin. *Methods Enzymol.* 184: 51–67.

Hutter, J. L., and J. Bechhoefer. 1994. Calibration of atomic-force microscope tips. *Rev. Sci. Instrum.* 64:1868–1873.

Israelachvili, J. N. 1992. Intermolecular and Surface Forces, 2nd ed. Academic Press, London.

Johnson, K. L., K. Kendall, and A. D. Roberts. 1971. Surface energy and the contact of elastic solids. *Proc. R. Soc. Lond. Ser. A.* 324:301–313.

Kuo, S. C., and D. A. Lauffenburger. 1993. Relationship between receptor/ligand binding affinity and adhesion strength. *Biophys. J.* 65:2191–2200.

Lauffenburger, D. A., and A. F. Howitz. 1996. Cell migration: a physically integrated molecular process. *Cell.* 84:359–369.

Lawrence, M. B., and T. A. Springer. 1991. Leukocytes roll on a selectin at physiologic flow rates: distinction from and prerequisite for adhesion through integrins. *Cell.* 65:859–873.

Leckband, D. E., F.-J. Schmitt, J. N. Israelachvili, and W. Knoll. 1994. Direct force measurements of specific and nonspecific protein interactions. *Biochemistry.* 33:4611–4624.

Lee, G. U., D. A. Kidwell, and R. J. Colton. 1994. Sensing discrete streptavidin-biotin interactions with AFM. *Langmuir.* 10:354–361.

Livnah, O., E. A. Bayer, M. Wilchek, and J. L. Sussman. 1993. Three-dimensional structures of avidin and the avidin-biotin complex. *Proc. Natl. Acad. Sci. USA.* 90:5076–5080.

Lollo, B. A., K. W. H. Chan, E. M. Hanson, V. T. Moy, and A. A. Brian. 1993. Direct evidence for two affinity states for lymphocyte function-associated antigen 1 on activated cells. *J. Biol. Chem.* 268:21693–21700.

Moy, V. T., E.-L. Florin, and H. E. Gaub. 1994. Adhesive forces between ligand and receptor measured by AFM. *Colloids and Surfaces.* 93: 343–348.

Nicholson, M. W., A. N. Barclay, M. S. Singer, S. D. Rosen, and P. van der Merwe. 1998. Affinity and kinetic analysis of L-selectin (CD62L) binding to glycosylation-dependent cell-adhesion molecule-1. *J. Biol. Chem.* 273:763–770.

Rädler, J., and E. Sackmann. 1992. On the measurement of weak repulsive and frictional colloidal forces by reflection interference contrast microscopy. *Langmuir.* 8:848–853.

Radmacher, M., M. Fritz, C. M. Kacher, J. P. Cleveland, and P. K. Hansma. 1996. Measuring the viscoelastic properties of human platelets with the atomic force microscope. *Biophys. J.* 70:556–567.

Sano, T., and C. R. Cantor. 1995. Intersubunit contacts made by tryptophan 120 with biotin are essential for both strong biotin binding and biotin-induced tighter subunit association of streptavidin. *Proc. Natl. Acad. Sci. USA.* 92:3180–3184.

Schneck, J., W. L. Maloy, J. E. Coligan, and D. H. Margulies. 1989. Inhibition of an allospecific T cell hybridoma by soluble class I proteins and peptides: estimation of the affinity of a T cell receptor for MHC. *Cell.* 56:47–55.

Springer, T. A. 1990. Adhesion receptors of the immune system. *Nature.* 346:425–434.

Springer, T. A. 1994. Traffic signals for lymphocyte recirculation and leukocyte emigration: the multistep paradigm. *Cell.* 76:301–314.

Sung, K. L., P. Kuhlman, F. Maldonado, B. A. Lollo, S. Chien, and A. A. Brian. 1992. Force contribution of the LFA-1/ICAM-1 complex to T cell adhesion. *J. Cell Sci.* 103:259–266.

Tözeren, A., L. H. Mackie, M. B. Lawrence, P. Y. Chan, M. L. Dustin, and T. A. Springer. 1992. Micromanipulation of adhesion of phorbol 12-myristate-13-acetate-stimulated T lymphocytes to planar membranes containing intercellular adhesion molecule-1. *Biophys. J.* 63:247–258.

Weber, P. C., D. H. Ohlendorf, J. J. Wendoloski, and F. R. Salemme. 1989. Structural origins of the high-affinity biotin binding to streptavidin. *Science.* 243:85–88.